D_4-Symmetric Dirhodium Tetrakis(binaphthylphosphate) Catalysts for Enantioselective Functionalization of Unactivated C–H Bonds

Ziyi Chen[1], Kristin Shimabukuro[1], John Bacsa[1], Djamaladdin G. Musaev*[,1,2] and Huw M. L. Davies*[,1]

[1]Department of Chemistry, Emory University, 1515 Dickey Drive, Atlanta, 30322, Georgia, USA

[2]Cherry L. Emerson Center for Scientific Computation, Emory University, 1521 Dickey Drive, Atlanta, Georgia 30322, United States

ABSTRACT: Dirhodium tetrakis(2,2'-binaphthylphosphate) catalysts were successfully developed for asymmetric C–H functionalization with trichloroethyl aryldiazoacetates as the carbene precursors. The 2,2'-binapthylphosphate (BNP) ligands were modified by introduction of aryl and/or chloro functionality at the 4, 4', 6, 6' positions. As the BNP ligands are C_2-symmetric, the resulting dirhodium tetrakis(2,2'-binaphthylphosphate) complexes were expected to be D_4-symmetric, but X-ray crystallographic and computational studies revealed this is not always the case because of internal T-shape CH-π and aryl-aryl interactions between the ligands. The optimum catalyst is Rh_2(*S*-megaBNP)$_4$, with 3,5-di(tert-butyl)phenyl substituents at the 4, 4' positions and chloro substituents at the 6, 6' positions. This catalyst adopts a D_4-symmetric arrangement and is ideally suited for site-selective C–H functionalization at unactivated tertiary sites with high levels of enantioselectivity (up to 99% ee), outperforming the best dirhodium tetracarboxylate catalyst developed for this reaction. The standard reactions were conducted with a catalyst loading of 1 mol % but lower catalysts loadings can be used if desired, as illustrated in the C–H functionalization of cyclohexane in 91% ee with 0.0025 mol % catalyst loading (29,400 turnover numbers). These studies further illustrate the effectiveness of donor/acceptor carbenes in site selective intermolecular C–H functionalization and expand the toolbox of catalysts available for catalyst-controlled C–H functionalization.

Introduction

Homoleptic chiral dirhodium tetracarboxylates have been shown to be tremendously effective catalysts, especially for carbene and nitrene transfer reactions.[1-4] Depending on the nature of the chiral ligands, they can self-assemble during formation of the dirhodium complexes to generate catalysts with higher symmetry than the ligands themselves, either C_2, C_4 or D_2 symmetric as illustrated in Figure 1A.[2,3] As the catalysts have two rhodium coordination sites, the high symmetry arrangement is advantageous because it would limit the number of different orientations when the carbene binds to the dirhodium complex. We and others have designed a wide range of high symmetry dirhodium tetracarboxylate catalysts[2-4] that have shown broad applicability in the reactions of donor/acceptor[1a-c, 2, 3] and donor/donor carbenes.[1d, e] Our most recent work has focused on C_4 symmetric bowl-shaped catalysts, which require blocking of one of the rhodium coordination sites to make them effective chiral catalysts.[3k, 4b] Therefore, we decided to explore whether appropriately designed C_2-symmetric binaphthylphosphate (BNP) ligands,[5] which would be expected to generate Rh_2(BNP)$_4$ complexes of D_4 symmetry with both rhodium sites being identical (Figure 1B), would have distinctive characteristics and broaden the scope of enantioselective C–H functionalization reactions. In this paper, we describe a new binaphthylphosphate dirhodium catalyst, Rh_2(*S*-megaBNP)$_4$ (*S*-**1**) (Figure 1C) and demonstrate that even though its conformational mobility is more complex than had been anticipated, it is very effective for asymmetric C–H functionalization with donor/acceptor carbenes.

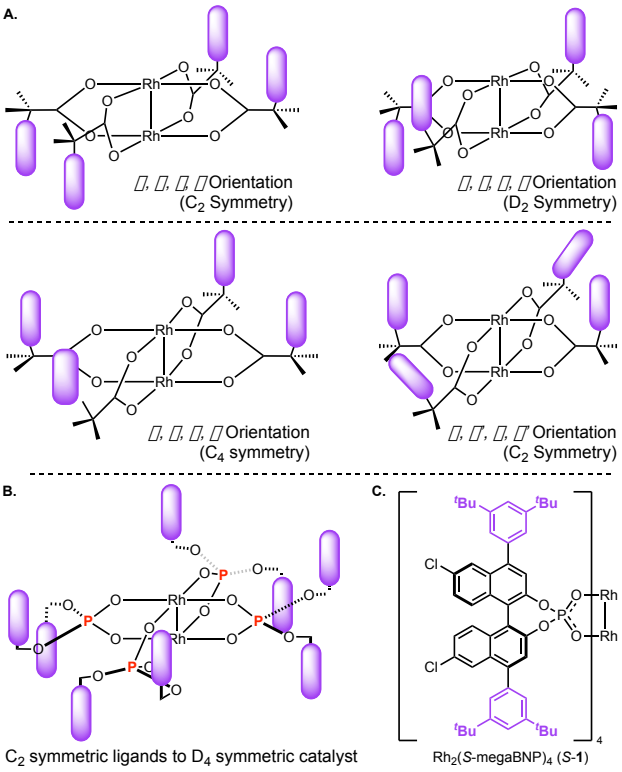

Figure 1. **A**. High symmetry orientations of dirhodium tetracarboxylates. **B**. Model of D_4 symmetric arrangement with C_2-symmetric phosphate ligands. **C**. Structure of the optimum catalyst, Rh_2(*S*-megaBNP)$_4$

The use of chiral binaphthylphosphate ligands in dirhodium catalysis started in the early 1990's,[6] but their application is far less developed compared to the dirhodium tetracarboxylate and carboxamidate catalysts.[1-4] A few examples are known where reasonably high levels of asymmetric induction were achieved but the scope of these reactions is limited. Figure 2 illustrates the most significant catalysts that have been developed.[6a, 7] In the pioneering studies by Pirrung,[6a] the parent Rh_2(*S*-BNP)$_4$, ***S*-2,** complex was shown to be capable of up to 50% ee in cycloaddition reactions (Figure 2). Later studies by Davies showed that in the cyclopropanation reactions with aryldiazoacetates, *R*-**2** is capable of relatively high levels of asymmetric induction but only when methoxy substituents were present in the aryl ring.[7p] The main challenge associated with the binaphthylphosphate ligands is how to modify their structure to enhance the asymmetric induction exhibited by the dirhodium catalysts. Typically, when dirhodium complexes of binaphthylphosphonic acids themselves are used as chiral protic catalysts, far superior performances can be obtained when bulky substituents are introduced at 3,3' positions in the binaphthyl.[8] However, introduction of bulky substituents at this position is not feasible for these dirhodium complexes because the C3-substituents of one ligand will sterically interfere with the adjacent ligand. Consequently, the dirhodium tetrakis-binaphthylphosphate catalysts can only be formed when the C3 substituent is either hydrogen or methyl, and the yield for formation of the C3 methyl-substituted complex *S*-**3** is very low (7%).[7o] Another option is to use partially hydrogenated ligands but catalyst *R*-**4a** still gives only moderate levels of asymmetric introduction (up to 44% ee).[7f] To date, the most promising studies are those by Hodgson who examined asymmetric cycloaddition of oxonium ylides derived from the dirhodium(tetra-binaphthylphosphate)-carbene intermediates. The Rh_2[*S*-4,4',6,6'-tetra-*N*-octyl-BNP]$_4$ catalyst *S*-**5**, with bulky *N*-octyl substituents, designed for increased solubility,[7e,7l] similar to the tactic used with the dirhodium tetraprolinate catalysts,[3b] performs well in enantioselective cycloaddition reactions, resulting in up to 86% (92%) ee.[7l] However, the corresponding tetraphenyl catalyst *S*-**6a**, which is closely related to the current catalyst design, results in much lower levels of enantioselectivity (11% ee), although the p-n-butylphenyl derivative *S*-**6b** gave up to 63% ee.[7e] It should be noted that another C_2 symmetric phosphate ligand class that have been successfully applied to generate D_4-symmetric dirhodium catalysts are the spiro ligands developed by Zhou,[9] but we decided to focus on binaphthylphosphates because of their ease of synthesis.

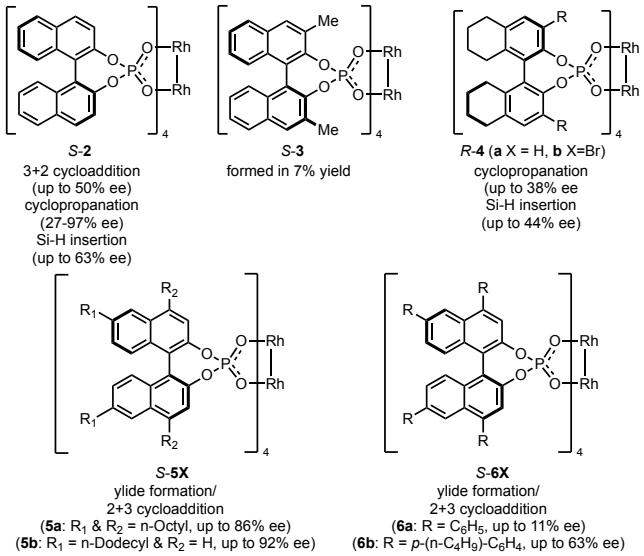

Figure 2. Representative examples of previously studied dirhodium tetrakis(binaphthylphosphonate) catalysts (*R*-**X** or *S*-**X**, depending on which enantiomer of the ligand is used)

In order for the dirhodium tetrakis(binaphthylphosphate) catalysts to match the range of highly asymmetric transformations possible with dirhodium tetracarboxylates, we reasoned that further ligand optimization is needed. The X-ray crystallographic structure (Figure 3) [7f] and our computational studies (see Figure S7.2) of Rh_2(*R*-BNP)$_4$, *R*-**2** indicate that this complex adopts a structure that is D_4 symmetric. This complex, however, has a relatively flat structure, with no major components of the ligands pointing directly towards the carbene binding site, which may explain why the asymmetric induction with *R*-**2** is typically modest. Therefore, we decided to explore whether introduction of large functionality into the BNP ligands would improve the asymmetric induction exhibited by this class of catalysts. As mentioned above, large functionality at C3 of the naphthyl group (color coded blue) cannot be accommodated because groups at this position would interfere with the adjacent ligands. The C4 position (colored green) appears best for introduction of sterically influencing groups, whereas the C6 position (colored yellow) is too far away from the rhodium. Even substituents at C4 would need to be large because it is still located relatively far away from the rhodium coordination site. On the basis of this initial analysis, the tetraphenyl derivative *S*-**6a** appeared to be a promising starting point because the phenyl groups are highly

amenable for modification into larger groups by means of metal-catalyzed cross coupling reactions. Therefore, we decided to begin our studies by evaluating *S*-**6a** in a standard C–H functionalization reaction as a reference reaction and then analyze its structure to understand its limitations. Then, we examined a series of more bulky derivatives, following our central hypothesis that bulky C4 substituents would be a requirement for enhanced enantioselectivity.

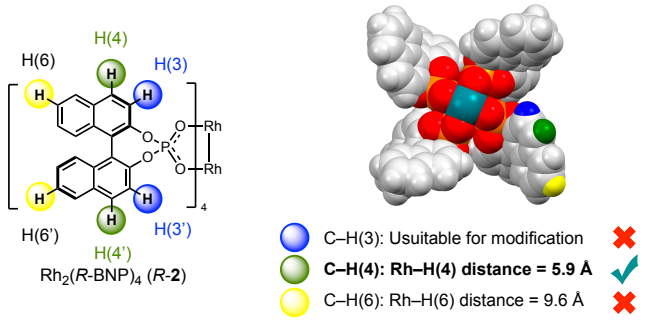

Figure 3. Rationale for catalysts optimization studies illustrated on X-ray structure of *R*-**2**

Results and Discussion

The synthetic route to a series of the 4,4',6,6'-tetraarylbinaphthylphosphate catalysts is summarized in Scheme 1, following an adapted procedure to the one that been used previously for the synthesis of tetraphenyl derivative *S*-**6a**.[7e] Bromination of the binaphthyl ether *S*-**7** preferentially occurs at the 6,6' positions but the 4,4' position can also be brominated under more forcing conditions to generate the tetrabromo derivative *S*-**8**. Tetra-fold Suzuki coupling on *S*-**8** generated a series of tetraaryl derivatives *S*-**9a, c**, **d**, which on de-etherification to form *S*-**10a, c**, **d** , followed by generation of the phosphonic acid *S*-**11a, c**, **d** and ligand exchange with dirhodium tetraacetate, generated the desired binaphthylphosphate catalysts *S*-**6a, c**, **d** .

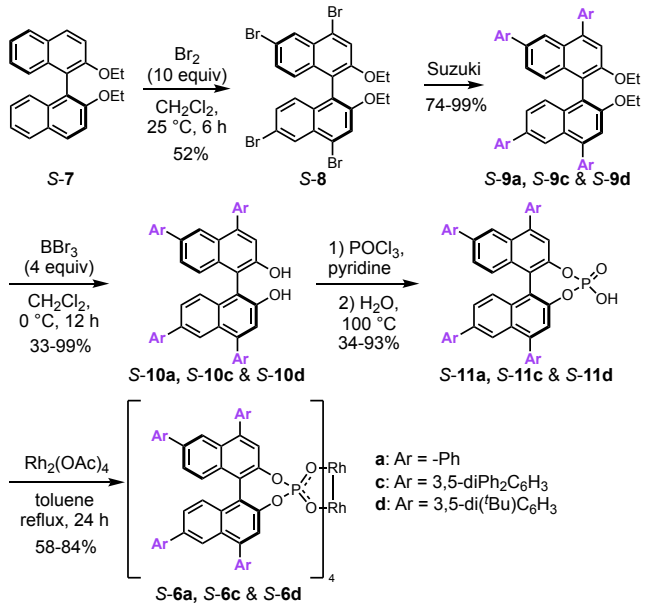

Scheme 1. Synthesis of tetra-arylbinaphthylphosphate catalysts *S*-6a, c, d.

The binaphthylphosphate catalysts *S*-**2**, *S*-**6a,** *S*-**6c** and *S*-**6d** were tested for their effectiveness at asymmetric induction in a standard C–H functionalization of cyclohexane using the bromoaryldiazoacetate **12a** as the carbene source to form the functionalized product **13a**.[10] The parent catalyst *S*-**2** generated **13a** in only 27% ee, while the previously known tetraphenyl catalyst *S*-**6a**[7e] gave **13a** in 44% ee. Gratifyingly, a significant enhancement was obtained with the 3,5-disubstituted aryl catalysts *S*-**6c** and *S*-**6d**, which generated **13a** in 79% ee and 85% ee, respectively.

Table 1. Initial catalyst screening of C–H functionalization of cyclohexane[a]

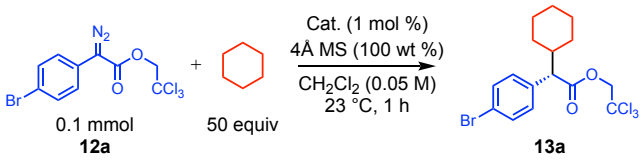

Entry	Catalyst	NMR yield[b] (%)	ee (%)
1	*S*-**2**	54	**27**
2	*S*-**6a**	69	**44**
3	*S*-**6c**	69	**79**
4	*S*-**6d**	61	**85**

[a]Reaction conditions: catalyst (1 mol %), cyclohexane (50 equiv), 4Å MS (100 wt %), 1 mL CH_2Cl_2 in a 4 mL vial, diazo (0.1 mmol) in 1 mL CH_2Cl_2 was added over 1 h via syringe pump at 23 °C. The ee values were determined by chiral HPLC analysis. [b]NMR yields were determined with trichloroethylene as internal standard (6.47 ppm)

Even though the enantioselectivity in the C–H functionalization improved with increasing the size of the aryl-substituent on the catalyst, the results are still below what would have been possible with the chiral dirhodium tetracarboxylate catalysts.[10] To gain further insight about these catalysts, we prepared suitable crystals of the tetraphenyl catalyst *S*-**6a** for X-ray crystallographic analysis. At the onset of this work, we expected all the catalysts to adopt a D_4-symmetric orientation, as had been reported for the parent catalyst, *S*-**2**,[7f] but this was definitely not the case for *S*-**6a**. The unit cell contained three molecules of *S*-**6a** and they were in different conformations, none of which had D_4 symmetry (Figure 4). This result indicates that the expectation that all the catalysts would routinely be D_4 symmetric is not a given outcome.

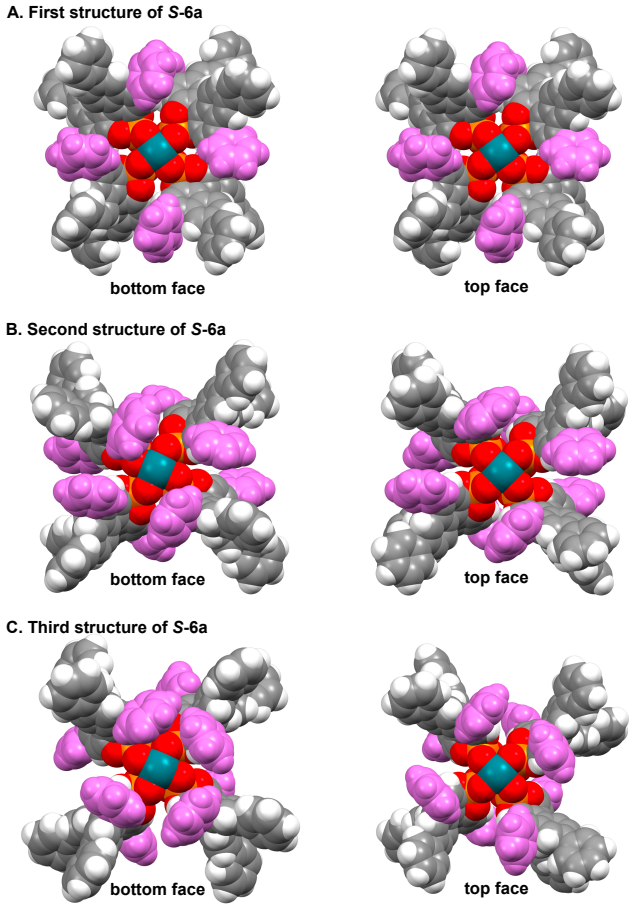

Figure 4. Three distinct conformers of *S*-**6a** in the crystal structure unit cell. Two views from of each conformer is given (the 4,4'-phenyl substituents are colored in purple to enhance the visualization). None of the conformers are in a high symmetry arrangement.

The unexpected variability in how the BNP ligands of *S*-**6a** orientate themselves in the crystal packing would likely also influence the catalyst structure in solution. In order to evaluate this expectation, we carried out computational studies on *S*-**6a** and its various derivatives (see below, and Supporting Information). These calculations were conducted at the {[B3LYP-D3(BJ)] + PCM(DCM)}/[6-31G(d,p) + Lanl2dz] level of theory (see the Supporting Information for details).[11,12] The calculations on *S*-**6a** converged to the structure shown in Figure 5. As seen from this figure, the calculated structure of *S*-**6a** is not D_4 symmetric and exhibits several T-shape CH-π and π-π interactions between the Ph-rings, as well as the Rh-π(Ph) interactions which results in closing of one side of the catalyst versus the other site, and decreasing symmetry of the catalyst to either C_2 (Figure 4A) or no simplified symmetry at all (Figure 4B and 4C). The calculated bowl widths are 6.7 and 18.0 Å for the top- and bottom-side of the catalyst *S*-**6a**, respectively (see Figure 5). Interestingly, the use of B3LYP instead of the B3LYP-D3BJ approach reduces the difference between the top- and bottom-site bowl-width of catalyst *S*-**6a** from 11.3 to 3.3 Å (the B3LYP calculated top-site and bottom-site bowl-width are 12.0 and 15.3 Å, respectively). Comparison of the above presented findings at the B3LYP and B3LYP-D3BJ levels of theory, illustrates the critical importance of weak interaction in defining the structure of the Rh_2(*R*-tetraarylbinaphthylphosphate) complexes,[13] and the structural flexibility of the BNP ligands in *S*-**6a** (for details, see the supporting information, Figure S7.6). We also used computation to explore whether the 6,6' phenyl groups in *S*-**6a** have a major influence on the catalyst structure and found that the unsubstituted 6,6'-H and 6,6'-Cl substituted analogs of this catalyst adopt an almost identical orientation to *S*-**6a** (see the Supporting Information for details, Figures S7.4 and S7.8).

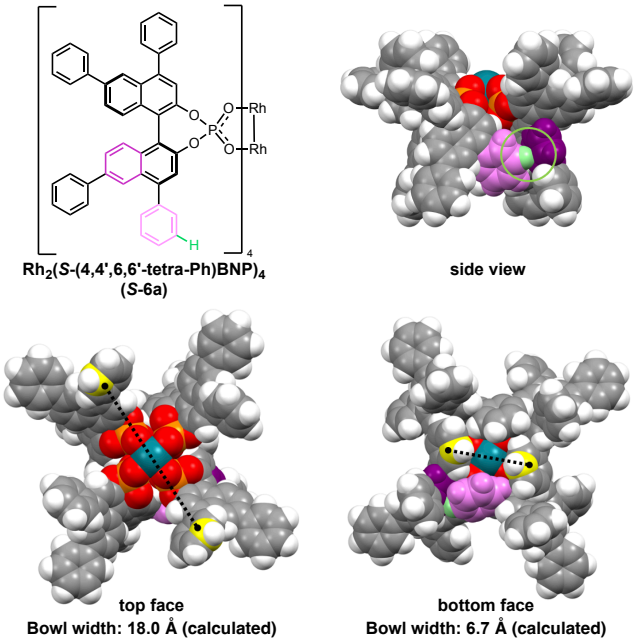

Figure 5. Computationally minimized structure of *S*-**6a** showing evidence of T-shape CH-π interaction, which disrupts the expected D_4 symmetry of the catalysts. Bowl width values are measured across the catalyst bowl between the innermost *meta*-positioned carbon atoms (yellow) of the 4,4'-aryl substituents.

The computational studies show that the 4,4'-diaryl substituents play a pivotal role in determining whether the catalysts adopt a high symmetry structure and the 6,6' substitutions have limited effect. Therefore, we decided to adjust the design of the next catalysts to focus on bulky 4,4'-diaryl substituents, while maintaining the same groups at the 6,6' positions. The direct synthesis of 4,4' disubstituted binaphthols with no substituents at the 6,6' position is challenging because the 6,6' positions are favored for electrophilic aromatic substitution.[7b-e] Therefore, we embarked on the synthesis of binaphthylphosphate catalysts with bulky aryl substituents at C4, C4' and smaller chlorine substituents at the C6, C6', as illustrated in Scheme 2. Bromination of *S*-**7** under mild conditions[7b-d] resulted in the selective formation of the 6, 6'-dibromo derivative *S*-**14**. Treatment of *S*-**14** with copper(I) chloride generated the 6,6'-dichloro derivative *S*-**15**,[14] which then could be dibrominated at the 4, 4' positions to form *S*-**16**. Double Suzuki coupling of *S*-**16** only occurred at the bromide and subsequent reactions that were used in Scheme 1, generated the desired ligands *S*-**17a** and *S*-**17b** with 4,4'-aryl substituents. The ligand exchange with dirhodium tetraacetates generated the desired catalysts *S*-**18** and Rh_2(*S*-megaBNP)$_4$ (*S*-**1**). Although, the initial plan was to prepare a library of catalysts in this series, the excellent performance of *S*-**1** precluded the necessity to prepare an extended library.

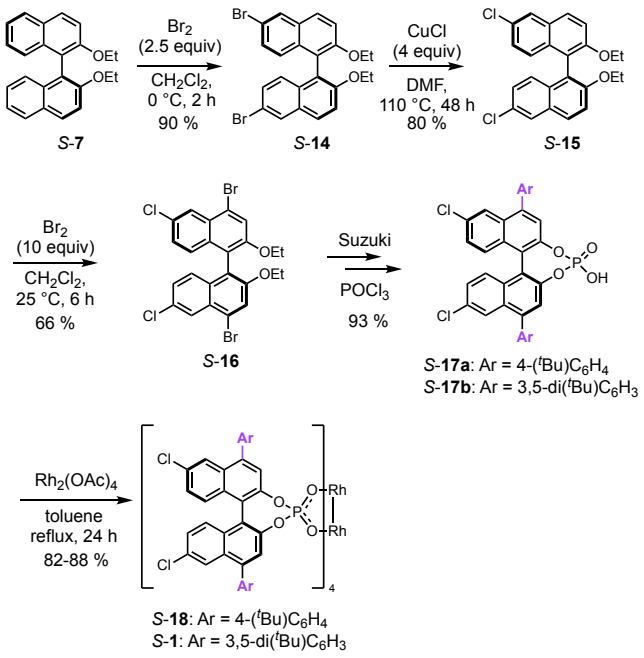

Scheme 2. Synthesis of the Rh_2-[6,6'-dichloro-4,4'-diarylbinaphthylphosphate] catalysts *S*-18 and Rh_2(*S*-megaBNP)$_4$ (*S*-1).

The two new catalysts were evaluated in the standard C–H functionalization with cyclohexane and the results are summarized in Table 2. The *para*-tert-butylphenyl derivative *S*-**18** was an effective catalyst but the enantioselectivity during the formation of **13a** remained moderate (54% ee). In contrast, the 3,5-di-tert-butylphenyl catalyst *S*-**1** was exceptional, generating **13a** in 99% ee. In these initial studies, a vast excess of cyclohexane was used, but the reaction was still very effective with just 10 equiv of cyclohexane, generating **13a** in 85% isolated yield and 99% ee.

Table 2. C–H functionalization of cyclohexane using *S*-18 and *S*-1 as catalysts [a]

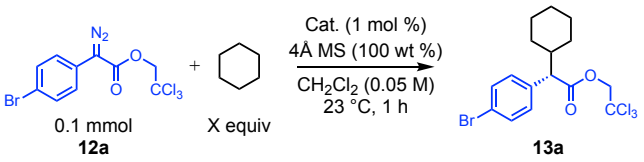

Entry	Catalyst	X equiv	NMR yield[c] (%)	ee (%)
1	*S*-**18**	50	72	54
2	*S*-**1**	50	94	99
3[b]	*S*-**1**	**10**	**94(85**[d]**)**	**99**

[a]Reaction conditions and analysis were the same as described in Table 1. [b]0.5 mol % catalyst was used. [c]NMR yields were determined with trichloroethylene as internal standard (6.47 ppm). [d]Isolated yield.

The difference in enantioselectivity observed with catalysts *S*-**18** and *S*-**1** is dramatic and so, further structural analyses of these catalysts were performed to understand what were the stereochemical controlling factors. X-ray and computational (see the supporting Information, Figure S7.10 for details) studies of *S*-**18** (see Figure 6) show that it has a more ordered ligand orientation than the tetraphenyl catalyst *S*-**6a** but it still does not adopt a D_4 symmetric structure. Instead, it adopts a C_4 symmetry. One face of the catalyst has the four tert-butyl-phenyl groups attracted towards each other (structure **D**), with a bowl-width of 9.7 Å (the calculated value is 10.4 Å), whereas on the other face (structure **E**) four tert-butyl-phenyl groups are spread apart with a bowl-width of 14.3 Å (the calculated value is 17.7 Å), Thus, one face (structure **E**) of catalyst *S*-**18** is quite open and the other face (structure **D**) is still relatively closed. In other words, either the catalyst will have two distinctive faces for carbene binding and/or the ligands will have conformational mobility between the two structures. In either case, the overall effect is that this catalyst would not have a well-defined orientation for the carbene coordination, and this is presumably reflected in the moderate enantioselectivity it exhibited.

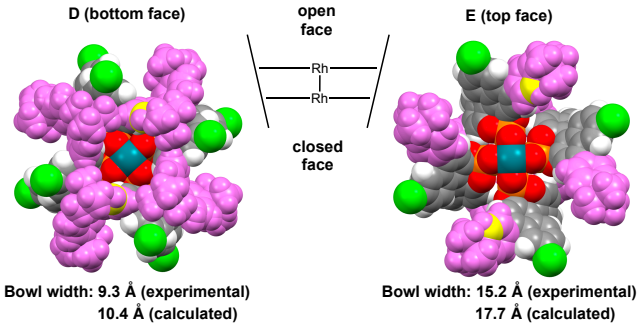

Figure 6. C_4-Symmetric crystal structure of *S*-**18** showing a bottom view **D** and a top view **E** (the 4,4'-aryl substituent is colored in purple to enhance the visualization). One face of the catalyst is open and the other is closed. Bowl width values are measured across the catalyst bowl between the innermost *meta*-positioned carbon atoms (yellow) of the 4,4'-aryl substituents.

In contrast to the results above, the X-ray structure of the optimum catalyst, Rh_2(*S*-megaBNP)$_4$ (*S*-**1**) indicates that it adopts a D_4 symmetric arrangement (Figure 7). The sterically more demanding 3,5-di-tert-butylphenyl does not appear to accommodate closer approach of this functionality on one face of the catalyst versus the other and hence both faces of the catalysts are identical. DFT structural optimization studies were conducted, starting from the X-ray structure of *S*-**1**, but the structure remained virtually unchanged (see the supporting Information, Figure S12 for details). This indicates that the solid-state orientation is likely to be the same in solution. Due to the high symmetry, the four potential binding orientations for each face of the catalyst are identical (or almost identical), which leads to a greater likelihood for the catalyst to be capable of achieving high asymmetric induction. Furthermore, the C_4 or D_4 symmetry of catalysts *S*-**18** and Rh_2(*S*-megaBNP)$_4$ (*S*-**1**), support the hypothesis that having large aryl groups at the 4,4' positions favor organization of the complex in a high symmetry orientation.

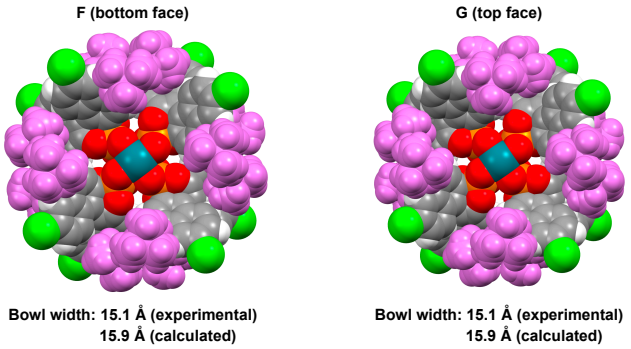

Figure 7. D_4-Symmetric crystal structure of *S*-**1** showing a bottom view **F** and a top view **G** (the 4,4'-aryl substituent is colored in purple to enhance the visualization). Bowl width values are measured across the catalyst bowl between the innermost *meta*-positioned carbon atoms (yellow) of the 4,4'-aryl substituents.

Even though the X-ray crystallographic and computational studies of Rh_2(*S*-megaBNP)$_4$ (*S*-**1**) indicated that it maintains a D_4 symmetric structure, the proton NMR spectrum indicated that *S*-**1** has hindered conformational mobility. This can be readily seen by comparing the NMR spectra of the ligand *S*-**17b** and catalyst *S*-**1** (Figure 8). The proton NMR signals for the ligand are sharp, whereas the signals for the catalyst are broad, indicating the existence of significant conformational barriers. Furthermore, there are some major changes in the chemical shifts with some signals de-shielded, most notably the tert-butyl group from 1.4 ppm in the ligand **17b** to two signals at 1.3 and 0.9 ppm in the complex *S*-**1**. Therefore, further NMR studies were conducted to determine whether the solid-state structure of *S*-**1** was a realistic view of the solution structure, or whether other hindered rotation issues were in play.

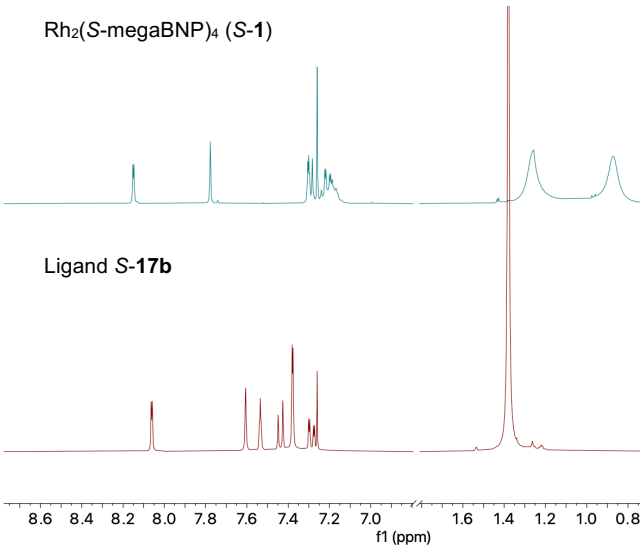

Figure 8. Proton NMR of catalyst Rh_2(*S*-megaBNP)$_4$ (*S*-**1**) and ligand *S*-**17b**. When the complex *S*-**1** is formed, the spectra are considerably broadened and the signals for the tert-butyl groups occur at 1.2 and 0.8 ppm, with one of them considerably shielded.

Variable NMR studies revealed that the conformational barrier was about 13 kcal/mol (see supporting information, Figure S6.1 for the details of the variable temperature NMR experiments). In order to determine what was likely causing the conformational barrier NOE studies were conducted (see supporting information, Figures S6.3-S6.6 for details). Of particular significance to this analysis was the data obtained for the NOE exhibited by the tert-butyl groups as shown in Figure 9. In the free ligand *S*-**17b** the tert-butyl group had the expected positive NOE to the ortho-hydrogens on the benzene ring and the C3 and C5 hydrogens on the naphthyl ring. In the complex *S*-**1**, NOE enhancements were seen to these same aromatic protons but also to the C7 and C8 protons on the naphthyl ring, which should be too far removed from the tert-butyl group for NOE.

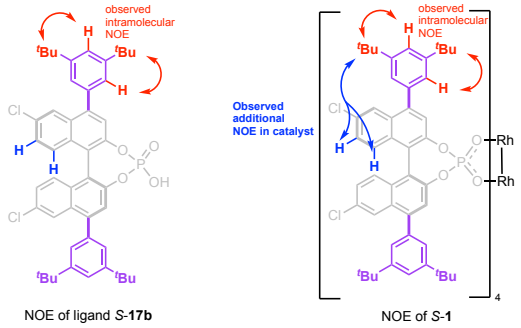

Figure 9. NOE enhancements observed in the ligand *S*-**17b** and catalyst *S*-**1**(see the Supplemental Information, Figures S6.1-S6.6) for the detailed spectral data).

On examining the crystal structure of *S*-**1**, it is clear that a tert-butyl group of one ligand, is closely aligned to the naphthyl ring of the adjacent ligand, and we propose that the catalyst in solution adopts a similar structure to the X-ray structure and the additional NOE's seen in **1** compared to the ligand are due to intermolecular interaction between the tert-butyl group and the adjacent ligands. Of particular significance is that both tert-butyl groups cause the NOE effect even though only one is in close proximity to the naphthyl group of the adjacent ligand. This would indicate that the hindered rotation is occurring between the binaphthyl and the di-tert-butylphenyl bond. The barrier for rotation is less in the ambient temperature NMR studies of the ligand *S*-**17b** but becomes greater in the complex *S*-**1** because of additional intermolecular interactions between the tert-butyl group of one ligand and the binaphthyl and the di-tert-butylphenyl fragments of adjacent ligands.

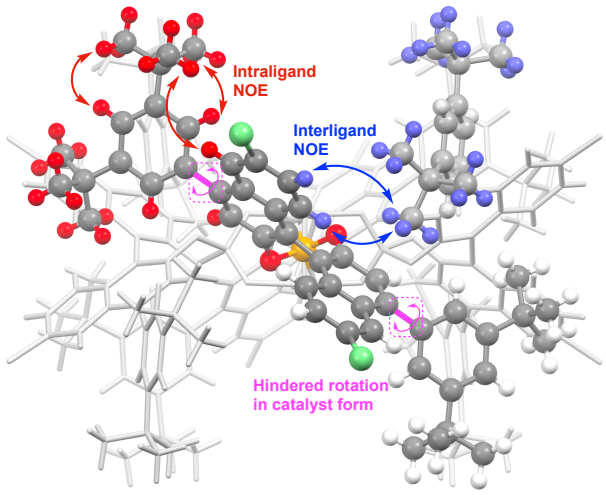

Figure 10. Key NOE enhancements between the tert-butyl groups and aromatic protons. Red arrows indicate NOE enhancement within the

same ligand. Blue arrows indicate NOE enhancement with protons in the adjacent ligands.

Having established that Rh_2(*S*-megaBNP)$_4$ (*S*-**1**) is the optimum catalyst and developed a reasonable understanding for why it is so effective, we then began to explore its synthetic potential in C–H functionalization reactions. The first series of experiments examined the influence of *p*-substituted aryldiazoacetates and a few heteroaryldiazoacetates on the enantioselectivity of the C–H functionalization reaction (Table 3). In general, with the dirhodium tetracarboxylates, we have found that donor/acceptor carbenes with trihaloethyl esters are better than those with a standard methyl ester in the functionalization of unactivated C–H bonds and often result in higher levels of enantioselectivity.[15] The reaction of aryldiazoacetates to form products **13a-c** compare the influence of the ester group on the reactions catalyzed by *S*-**1**. All three give effective transformations but the enantioselectivity with the trichloroethyl ester (99% ee) is higher than the methyl ester (90% ee) and the trifluoroethyl ester (91% ee). High enantioselectivity can be obtained when the *p*-substituent is electron withdrawing, as seen with **13d-f** (92-95% ee) but the trifluoromethanesulfonyl derivative does not do as well, forming **13g** in 78% ee. A *p*-phenyl substituent generates **13h** with high enantioselectivity (92% ee), but there is a slight drop with the *p*-toluyl derivative, forming **13i** in 86% ee. Other aromatic systems were also examined to form products **13j-l**. The 2-naphthyl and 4-chloropyridyl diazo derivatives perform well, forming **13j** in 90% ee and **13k** in 94% ee, respectively, but the chloropyrimidine derivative generated **13l** with only 64% ee. The diazo compounds that performed the worse were the ones with an electron donating methoxy group (61% ee, product **13m**), a bulky tert-butyl group (41% ee, product **13n**) and the parent phenyl derivative lacking a *para* substituent (56% ee, product **13o**).

Table 3. C–H functionalization of cyclohexane with *p*-substituted aryldiazoacetates [a]

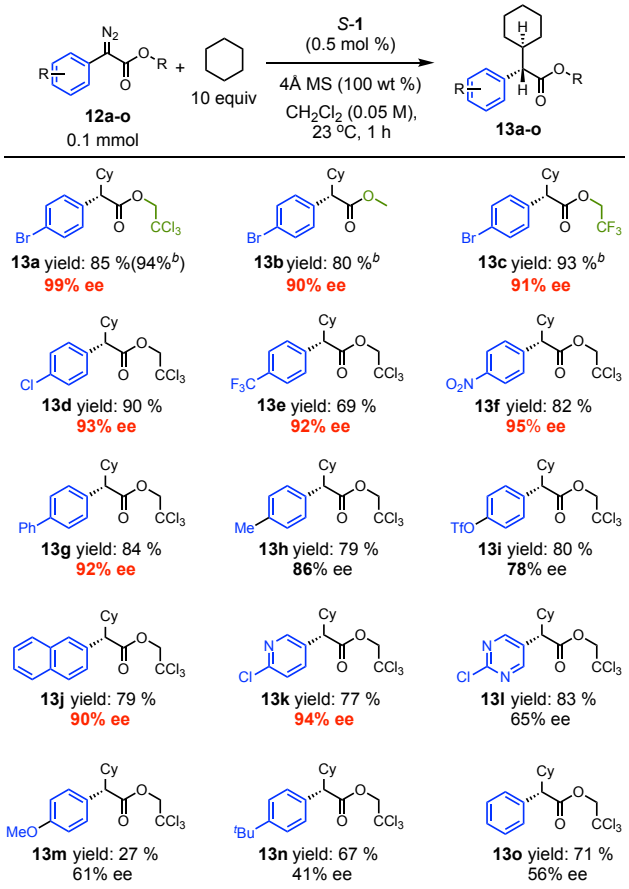

[a]Reaction conditions: catalyst (0.5 mol %), cyclohexane (10 equiv), 4Å MS (100 wt %), 1 mL CH_2Cl_2 in a 4 mL vial, diazo (0.1 mmol) in 1 mL CH_2Cl_2 was added over 1 h via syringe pump at 23 °C. Isolated yields were given. The ee values were determined by chiral HPLC analysis. [b]NMR yields were determined with trichloroethylene as internal standard (6.47 ppm)

The variable enantioselectivity, depending on the nature of the *para* substituent, lead to the hypothesis that even though the catalyst is likely to be D_4 symmetric in solution, it is still necessary for there to be a well-defined interaction between the *p*-substituted aryl group and the wall of the catalyst to lock the ligand/carbene interaction (Figure 11). As the aromatic rings in the catalyst are electron rich, it would be reasonable that the most effective aryl group on the carbene would be electron withdrawing. An aryl group plus the *para* substituent appears to be a requirement for an effective interaction with the catalyst not just a phenyl group. If the group is too large such as tert-butyl (**13n**) or is absent (**13o**), there is a considerable drop in the level of asymmetric induction. Computational studies were attempted on the structures of the carbene [both Ph-trichloroethyl and (*p*-Br)Ph–trichloroethyl] bound *S*-**1** complexes. These carbene complexes were too big for complete frequency analyses but their optimized structures (see the Supporting Information, Figure S7.14) show that the *para*-substituent causes the carbene to orientate itself between two adjacent ligands, whereas the orientation is not so stringent when an unsubstituted phenyl ring is present.

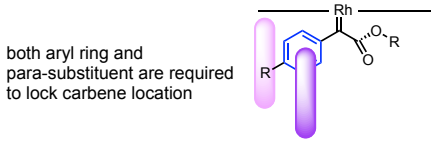

Figure 11. Working hypothesis – electron withdrawing para-substituted aryl rings are needed to lock the rhodium carbene in a defined position in the catalyst.

In order to test the working hypothesis further, control experiments were conducted with differentially substituted aryldiazoacetates. The reference substrate was the *p*-chloro derivative, which had been shown to generate **13d** in 93% ee (Table 4, entry 1). When the reaction was conducted on the *m*-chloro or *o*-chloro derivatives, the enantioselectivity was considerably lower (48% ee for **13p** and 60% ee for **13q**, respectively). Low enantioselectivity was also observed with a variety of *meta* substituents as shown in the formation of **13r-t** (18-49% ee). Interestingly, even though 3,5-dibromo derivative **13u** was formed with low levels on enantioselectivity (11% ee), the 3,4-dichloro and 3,4-dibromo derivatives, **13v** and **13w**, were both formed in 91% ee. These control studies further support the hypothesis that an aryl group with a *para*-substituent is a crucial component for achieving high asymmetric induction in the C–H functionalization reactions with *S*-**1**.

Table 4. Testing the working hypothesis with differentially substituted haloaryldiazoacetates[a]

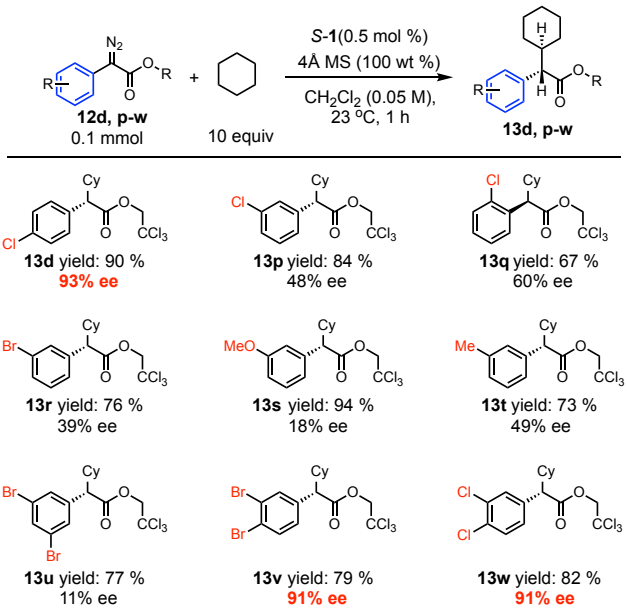

[a]Reaction conditions: catalyst (0.5 mol %), cyclohexane (10 equiv), 4Å MS (100 wt %), 1 mL CH_2Cl_2 in a 4 mL vial, diazo (0.1 mmol) in 1 mL CH_2Cl_2 was added over 1 h via syringe pump at 23 °C. Isolated yields were given. The ee values were determined by chiral HPLC analysis.

Having established that Rh_2(*S*-megaBNP)$_4$ (*S*-**1**) is capable of high levels of asymmetric induction, we then examined its influence on catalyst-controlled site-selective and enantioselective functionalization of unactivated C–H bonds. The dirhodium tetracarboxylate catalysts are capable of exceptional site selectivity and so, we decided to challenge *S*-**1** and see how it would compete against some of the best dirhodium tetracarboxylate catalysts. Pentane (**14**) and 2-methylhexane (**15**) were used as the two test substrates. The bulky D_2-symmetric catalyst, Rh_2(*R*-3,5-di(*p*-^{t}BuC$_6$H$_4$)TPCP)$_4$ (*R*-**23**), has been shown to drive the C–H functionalization of donor/acceptor carbenes towards the most accessible secondary C–H bond.[3i] In the case of pentane, a clean reaction occurs at C2, favoring **19**, with no observed reaction occurring at C3 to form **20**. The only regioisomer formed is a trace amount of C–H functionalization at the methyl group. Furthermore, the C–H functionalization to form **19** proceeds with 9:1 d.r. and in 99% ee. The reaction of pentane with *S*-**1**, as catalyst, gave a 14:1 site selectivity for C2 functionalization (**19**) over C3 functionalization (**20**), indicating that it is not as sterically demanding as Rh_2(R-3,5-di(*p*-^{t}BuC$_6$H$_4$)TPCP)$_4$ and thus, does not distinguish as well between the two methylene sites. Furthermore, the C2 diastereoselectivity for the formation of **19** is inferior (2:1 d.r) to the *R*-**23**-catalyzed reaction (9:1 d.r). The second comparison is against the best tertiary selective catalyst, Rh_2(S-TCPTAD)$_4$ (*S*-**24**). This catalyst is less sterically demanding than *R*-**23** and preferentially reacts at the most accessible tertiary C–H bond.[3j] The head-to-head comparison using 2-methylhexane (**15**) as substrate reveals that *S*-**1** competes very well with *S*-**24**. Not only does it give enhanced site selectivity for the tertiary site to preferentially form **21** over **22** (11:1 r.r. versus 5:1 r.r.) but the level of asymmetric induction at the tertiary group to form **21** is enhanced (91% ee for *S*-**1**, versus 77% ee for *S*-**24**).

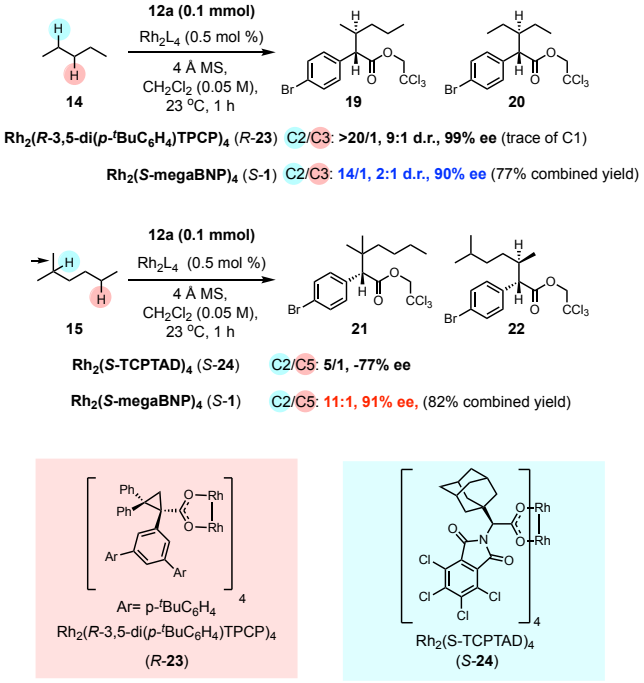

Scheme 3. Comparison of Rh_2(*S*-megaBNP)$_4$ (***S*-1**) with the established chiral dirhodium tetracarboxylate catalysts.

As Rh_2(*S*-megaBNP)$_4$ (*S*-**1**) competes well with *S*-**24** for site selective tertiary C–H functionalization, a detailed study was conducted on a range of substrates **25a-m** and the results are described in Table 5. The parallel reactions with Rh_2(*S*-TCPTAD)$_4$ are included in the Supporting Information for comparison purposes. The reactions were conducted under two reaction conditions. Condition A uses an excess of trap and this is very

effective for cheap volatile hydrocarbons. Condition B uses 2 equiv of the aryldiazoacetates and was preferred when more elaborate substrates were used. *S*-**1**-catalyzed reactions strongly prefer the most accessible tertiary C–H bonds (**25a-d**) although a readily accessible secondary C–H bond can still be a competitive site (**25b**). The reaction can be carried out in the presence of other functionality as illustrated with **25e-i**. Bromo, phthalimido, *p*-substituted phenoxy, and boronates are compatible with these reactions. In all cases, the enantioselectivity is high, ranging from 80-95% ee. The reaction can also be conducted on other cyclic substrates, as illustrated with **25j-l**. The reaction with adamantane is particularly impressive, as the C–H functionalization product **26l** is formed in 96% ee (entry 3).

Table 5. *S*-1–Catalyzed selective C–H functionalization at tertiary C–H bonds [a]

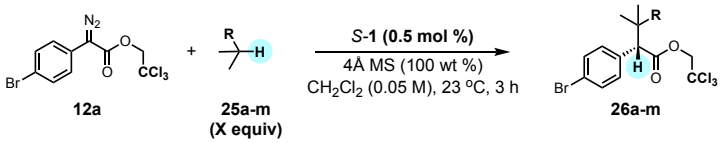

Entry	Substrate	Yield (%)	r.r.	ee (%)
a		75[a]	>20: 1	88
b		79[a]	9: 1 2°: 3°	90
c	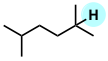	82[a]	>20: 1	89
d		59[a]	>20: 1	92
e		26[a] 58[b]	>20: 1 >20: 1	85 85
f	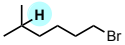	33[a] 72[b]	>20: 1 >20: 1	86 86
g	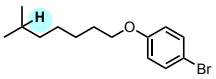	40[a] 66[b]	>20: 1 >20: 1	92 92
h	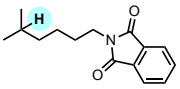	43[a] 73[b]	>20: 1 >20: 1	92 92
i	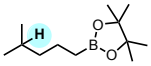	37[a] 43[b]	>20: 1 >20: 1	95 95
j		91[a]		98
k		80[a]		96
l		71[a]		96
26e =	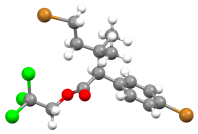 CCDC: 2335091			

Reactions conditions. [a]catalyst (0.5 mol %), **25a-f** and **25j-l** (1 mmol, 10 equiv) or **25g-i** (2 equiv), 4Å MS (100 wt %), 1 mL CH_2Cl_2 in a 4 mL vial, **12a** (0.1 mmol, 1 equiv) in 1 mL CH_2Cl_2 was added over 3 h via syringe pump at 23 °C. Isolated yields were given. The ee values were determined by chiral HPLC analysis. [b]catalyst (0.5 mol %), **25e-i** (0.1 mol, 1 equiv), 4Å MS (100 wt %), 1 mL CH_2Cl_2 in a 4 mL vial, **12a** (0.2 mmol, 2 equiv) in 1 mL CH_2Cl_2 was added over 3 h via syringe pump at 23 °C. Isolated yields were given. The ee values were determined by chiral HPLC analysis.

The dirhodium tetracarboxylate catalysts are capable of achieving very high turnover numbers (TONs) in the reactions of donor/acceptor carbenes.[10b,16] Therefore, we have conducted a brief study to evaluate the kinetic efficiency of *S*-**1** in the reaction of the aryldiazoacetate **12e** with cyclohexane. Previously we had shown that the optimum reaction conditions for high TON C–H functionalization with dirhodium tetracarboxylates were conducted at elevated temperature (60 °C) and used cyclohexane as solvent and an aryldiazoacetate with an electron withdrawing group on the aryl ring. Furthermore, the presence of small amount of DCC or DIC enhanced the TONs. As a test reaction, we conducted a reaction using the optimized conditions with a catalyst loading of 0.0025 mol %. Under these conditions, the C–H functionalization product **13e** was formed in 68% isolated yield (29,400 TON) and in 91% ee. This brief evaluation indicates that the phosphonate catalysts are capable of high TON's if desired.

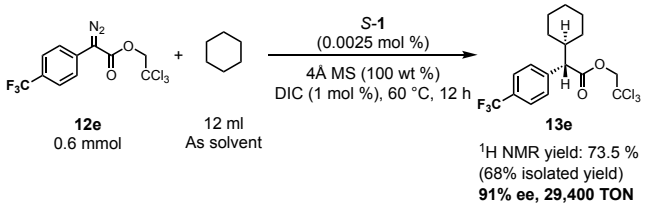

Scheme 4. Rh_2(*S*-megaBNP)$_4$ (*S*-1) catalyzed C–H functionalization under low catalyst loading.

In summary, we have prepared a series of chiral dirhodium tetrakis(binaphthylphosphate) catalysts and demonstrated their utility in site-selective and enantioselective functionalization of unactivated C–H bonds. At the onset of this work, all the catalysts were expected to be D_4-symmetric, but these studies revealed that this is not necessarily the case, The catalysts need to be carefully designed for them to adopt a D_4-symmetric structure and avoid symmetry-breaking T-shape CH-π interactions. Among these catalysts, Rh_2(*S*-megaBNP)$_4$ (*S*-**1**), displays excellent site-selectivity and enantioselectivity for functionalization of unactivated secondary and tertiary C–H bonds of cyclic alkanes and unactivated tertiary C–H bonds of various acyclic substrates. This work broadens the scope of chiral dirhodium catalysts capable of selective C–H functionalization by donor/acceptor carbenes.

ASSOCIATED CONTENT

Data Availability Statement

The data underlying this study are available in the published article and its online Supporting Information.

Supporting Information

The Supporting Information is available free of charge at XX

Complete experimental procedures, materials, computational details and findings, compound characterizations, and cartesian coordinates of all calculated systems (PDF).

CIF file of *S*-**6a** (CIF)

CIF file of *S*-**18** (CIF)

CIF file of *S*-**1** (CIF)

CIF file of **26e** (CIF)

Accession Codes

The following crystal structure has been deposited in the Cambridge Crystallographic Data Centre: Compound *S*-**6a** (CCDC 2349408), compound *S*-**18** (CCDC 2349403), compound *S*-**1** (CCDC 2349402) and compound **26e** (CCDC 2335091). These data can be obtained free of charge via www.ccdc.cam.ac.uk/data_request/cif, or by emailing data_request@ccdc.cam.ac.uk, or by contacting The Cambridge Crystallographic Data Centre, 12 Union Road, Cambridge CB2 1EZ, UK; fax: +44 902 1223 336033.

AUTHOR INFORMATION

Corresponding Author

Huw M. L. Davies – Department of Chemistry, Emory University, Atlanta, Georgia 30322, United States; https://orcid.org/0000-0001-6254-9398; Email: hmdavie@emory.edu

Djamaladdin G. Musaev – Cherry L. Emerson Center for Scientific Computation and Department of Chemistry, Emory University, Atlanta, Georgia 30322, United States; https://orcid.org/0000-0003-1160-6131; E-mail: dmusaev@emory.edu

Authors

Ziyi Chen – Department of Chemistry, Emory University, Atlanta, Georgia 30322, United States; https://orcid.org/0000-0002-8093-8466

Kristin Shimabukuro – Department of Chemistry, Emory University, Atlanta, Georgia 30322, United States; https://orcid.org/0000-0002-9543-6688

John Bacsa – Department of Chemistry, Emory University, Atlanta, Georgia 30322, United States

Author Contributions

The manuscript was written through contributions of all authors. All authors have given approval to the final version of the manuscript.

Funding Sources

The experimental work was supported by the National Institute of Health (GM099142) and the National Science Foundation (CHE-1956154). The computational work was supported by the National Science Foundation under the CCI Centre for Selective C–H Functionalization (CHE-1700982). Instrumentation used in this work was supported by the National Science Foundation (CHE 1531620 and CHE 1626172).

ACKNOWLEDGMENT

Constructive discussions within the Catalysis Innovation Consortium facilitated this study. At Emory University, we thank Dr. Bing Wang for NMR measurements, Dr. John Bacsa for X-ray structure determination, and Dr. Fred Strobel for MS measurements. The authors gratefully acknowledge the use of the resources of the Cherry Emerson Center for Scientific Computation at Emory University.

REFERENCES

(1) For general reviews on enantioselective carbene transformations, see: (a) He, Y.; Huang, Z. L.; Wu, K. K.; Ma, J.; Zhou, Y. G.; Yu, Z. K., Recent Advances in Transition-Metal-Catalyzed Carbene Insertion to C–H Bonds. *Chem. Soc. Rev.* **2022,** *51*, 2759- 2852. (b) Davies, H. M. L.; Morton, D. Guiding Principles for Site Selective and Stereoselective Intermolecular C–H Functionalization by Donor/Acceptor Rhodium Carbenes. Chem. Soc. Rev. 2011, 40, 1857-1869. DOI: 10.1039/c0cs00217h. (c) Cheng, S. Y.; Li, Q. Y.; Cheng, X. L.; Lin, Y. M.; Gong, L. Recent Advances in Asymmetric Transformations of Unactivated Alkanes and Cycloalkanes through Direct C–H Functionalization. Chin. J. Chem. 2022, 40, 2825-2837. (d) Huang, M. Y.; Zhu, S. F. Catalytic Reactions for Enantioselective Transfers of Donor-Substituted Carbenes. Chem Catalysis 2022, 2, 3112-3139. (e) Zhu, D.; Chen, L.; Fan, H.; Yao, Q.; Zhu, S. Recent Progress on Donor and Donor-Donor Carbenes. Chem. Soc. Rev. 2020, 49, 908-950. (f) Doyle, M. P.; Liu, Y.; Ratnikov, M. Catalytic, asymmetric, intramolecular carbon-hydrogen insertion. *Org. React.* **2013**, *80*, 1-131.

(2) (a) For reviews of high symmetry dirhodium tetracarboxylate catalysts, see: Davies, H. M. L.; Liao, K. Dirhodium Tetracarboxylates as Catalysts for Selective Intermolecular C–H Functionalization. *Nat. Rev. Chem.* **2019**, *3*, 347-360. (b) Hrdina, R. Dirhodium(II,II) Paddlewheel Complexes. *Eur. J. Inorg. Chem.* **2021**, *2021*, 501-528. (c) Hansen, J.; Davies, H. M. L. High Symmetry Dirhodium(II) Paddlewheel Complexes as Chiral Catalysts. *Coord. Chem. Rev.* **2008**, *252*, 545-555. (d) Adly, F. G. On the Structure of Chiral Dirhodium(II) Carboxylate Catalysts: Stereoselectivity Relevance and Insights. *Catalysts* **2017**, *7*, 347-365. Davies, H. M. L. Finding Opportunities from Surprises and Failures. Development of Rhodium-Stabilized Donor/Acceptor Carbenes and Their Application to Catalyst-Controlled C–H Functionalization. *J. Org. Chem.* **2019**, *84*, 12722-12745.

(3) For seminal studies on new classes of high symmetry dirhodium tetracaraboxylate catalysts, see: (a) Kitagaki, S.; Anada, M.; Kataoka, O.; Matsuno, K.; Umeda, C.; Watanabe, N.; Hashimoto, S.-I. Enantiocontrol in Tandem Carbonyl Ylide Formation and Intermolecular 1,3-Dipolar Cycloaddition of α-Diazo Ketones Mediated by Chiral Dirhodium(II) Carboxylate Catalyst. *J. Am. Chem. Soc.* **1999**, *121*, 1417-1418. (b) Davies, H. M. L.; Bruzinski, P. R.; Lake, D. H.; Kong, N.; Fall, M. J. Asymmetric Cyclopropanations by Rhodium(II) N-(Arylsulfonyl)Prolinate Catalyzed Decomposition of Vinyldiazomethanes in the presence of Alkenes. Practical Enantioselective Synthesis of the Four Stereoisomers of 2-Phenylcyclopropan-1-Amino Acid. *J. Am. Chem. Soc.* **1996**, *118*, 6897-6907. (c) Espino, C. G.; Fiori, K. W.; Kim, M.; Du Bois, J. Expanding the Scope of C–H Amination through Catalyst Design. *J. Am. Chem. Soc* **2004**, *126*, 15378-15379. (d) Liang, C.; Robert-Peillard, F.; Fruit, C.; Müller, P.; Dodd, R. H.; Dauban, P. Efficient Diastereoselective Intermolecular Rhodium-Catalyzed C–H Amination. *Angew. Chem. Int. Ed.* **2006**, *45*, 4641-4644. (e) DeAngelis, A.; Boruta, D. T.; Lubin, J.-B.; Plampin, J. N.; Yap, G. P. A.; Fox, J. M. The Chiral Crown Conformation in Paddlewheel Complexes. *Chem. Commun.* **2010**, *46*, 4541-4543. (f) Qin, C.; Davies, H. M. L. Role of Sterically Demanding Chiral Dirhodium Catalysts in Site-Selective C–H Functionalization of Activated Primary C–H Bonds. *J. Am. Chem. Soc.* **2014**, *136*, 9792-9796. (g) Liao, K.; Yang, Y.-F.; Li, Y.; Sanders, J. N.; Houk, K. N.; Musaev, D. G.; Davies, H. M. L. Design of Catalysts for Site-Selective and Enantioselective Functionalization of Non-Activated Primary C–H Bonds. *Nat. Chem.* **2018**, *10*, 1048-1055. (h) Liu, W.; Ren, Z.; Bosse, A. T.; Liao, K.; Goldstein, E. L.; Bacsa, J.; Musaev, D. G.; Stoltz, B. M.; Davies, H. M. L. Catalyst-Controlled Selective Functionalization of Unactivated C–H Bonds in the presence of Electronically Activated C–H Bonds. *J. Am. Chem. Soc.*

2018, *140*, 12247-12255. (i) Liao, K.; Negretti, S.; Musaev, D. G.; Bacsa, J.; Davies, H. M. L. Site-Selective and Stereoselective Functionalization of Unactivated C–H Bonds. *Nature* **2016**, *533*, 230-234. (j) Liao, K.; Pickel, T. C.; Boyarskikh, V.; Bacsa, J.; Musaev, D. G.; Davies, H. M. L. Site-Selective and Stereoselective Functionalization of Non-Activated Tertiary C–H Bonds. *Nature* **2017**, *551*, 609-613. (k) Fu, J.; Ren, Z.; Bacsa, J.; Musaev, D. G.; Davies, H. M. L. Desymmetrization of Cyclohexanes by Site- and Stereoselective C–H Functionalization. *Nature* **2018**, *564*, 395-399. (j) Chuprakov, S.; Kwok, S. W.; Zhang, L.; Lercher, L.; Fokin, V. V. Rhodium-Catalyzed Enantioselective Cyclopropanation of Olefins with N-Sulfonyl 1,2,3-Triazoles. *J. Am. Chem. Soc.* **2009**, *131*, 18034-18035.

(4) For recent examples of new high symmetry dirhodium tetracarboxylate catalysts, see: Bacher, E. P.; Twiringiyimana, R.; Rodriguez, K. X.; Wilson, R.; Bodnar, A. K.; O'Connell, R.; Toni, T. A.; Eckert, K. E.; Wiest, O.; Ashfeld, B. L. A Proline-Squaraine Ligand Framework (Pro-SqEB) for Stereoselective Rhodium(II)-Catalyzed Cyclopropanations. *Org. Lett.* **2023**, *25*, 8156-8161. (b) Garlets, Z. J.; Boni, Y. T.; Sharland, J. C.; Kirby, R. P.; Fu, J. T.; Bacsa, J.; Davies, H. M. L. Design, Synthesis, and Evaluation of Extended C_4-Symmetric Dirhodium Tetracarboxylate Catalysts. *ACS Catal.* **2022**, *12*, 10841-10848. (c) Brunard, E.; Boquet, V.; Saget, T.; Sosa Carrizo, E. D.; Sircoglou, M.; Dauban, P. Catalyst-Controlled Intermolecular Homobenzylic C(sp^3)–H Amination for the Synthesis of β-Arylethylamines. *J. Am. Chem. Soc.* **2024**, *146*, 5843-5854

(5) For reviews on binaphthylphosphates as ligands, see: Brodt, N.; Niemeyer, J. Chiral Organophosphates as Ligands in Asymmetric Metal Catalysis. *Org. Chem. Front.* **2023**, *10*, 3080-3109.

(6) (a) Pirrung, M. C.; Zhang, J. Asymmetric Dipolar Cycloaddition Reactions of Diazocompounds Mediated by a Binaphtholphosphate Rhodium Catalyst. *Tetrahedron Lett.* **1992**, *33*, 5987-5990. (b) McCarthy, N.; McKervey, M. A.; Ye, T.; McCann, M.; Murphy, E.; Doyle, M. P. A New Rhodium(II) Phosphate Catalyst for Diazocarbonyl Reactions Including Asymmetric Synthesis. *Tetrahedron Lett.* **1992**, *33*, 5983-5986.

(7) (a) M. Hodgson, D.; A. Stupple, P.; Johnstone, C. Efficient Rh(II) Binaphthol Phosphate Catalysts for Enantioselective Intramolecular Tandem Carbonyl Ylide Formation–Cycloaddition of α-Diazo-β-Keto Esters. *Chem. Commun.* **1999**, 2185-2186. (b) Hodgson, D. M.; Petroliagi, M. Rh(II)-Binaphthol Phosphate Catalysts in the Enantioselective Intramolecular Oxonium Ylide Formation–[3,2] Sigmatropic Rearrangement of α-Diazo-β-Ketoesters. *Tetrahedron: Asymmetry* **2001**, *12*, 877-881 (c) Hodgson, D. M.; Stupple, P. A.; Pierard, F. Y. T. M.; Labande, A. H.; Johnstone, C. Development of Dirhodium(II)-Catalyzed Generation and Enantioselective 1,3-Dipolar Cycloaddition of Carbonyl Ylides. *Chem. Eur. J.* **2001**, *7*, 4465-4476. (d) Hodgson, D. M.; Labande, A. H.; Pierard, F. Y. T. M.; Expósito Castro, M. Á. The Scope of Catalytic Enantioselective Tandem Carbonyl Ylide Formation–Intramolecular [3 + 2] Cycloadditions. *J. Org. Chem.* **2003**, *68*, 6153-6159. (e) Hodgson, D. M.; Selden, D. A.; Dossetter, A. G. Synthesis and Evaluation of 4,4′,6,6′-Tetrasubstituted Binaphtholphosphate Dirhodium(II) Complexes as Catalysts in Enantioselective Carbonyl Ylide Formation–Cycloaddition Reactions. *Tetrahedron: Asymmetry* **2003**, *14*, 3841-3849. (f) Hodgson, D. M.; Glen, R.; Redgrave, A. J. [3+2] Cycloaddition Reactions of Arylacetylenes with Carbonyl Ylides Derived from 1-Aryl-1-Diazohexane-2,5-Diones. *Tetrahedron Lett.* **2002**, *43*, 3927-3930. (g) Hodgson, D. M.; Glen, R.; Grant, G. H.; Redgrave, A. J. Catalytic Enantioselective [3+2]-Cycloadditions of Diazoketone-Derived Aryl-Substituted Carbonyl Ylides. *J. Org. Chem.* **2003**, *68*, 581-586. (h) Hodgson, D. M.; Labande, A. H.; Pierard, F. Extended Scope of Dirhodium(II)-Catalysed Enantioselective Intramolecular 1,3-Dipolar Cycloadditions of Carbonyl Ylides with Alkene and Alkyne Dipolarophiles. *Synlett* **2003**, 1, 59-62. (i) Hodgson, D. M.; Labande, A. H.; Pierard, F.; Castro, M. A. E. The Scope of Catalytic Enantioselective Tandem Carbonyl Ylide Formation-Intramolecular [3+2] Cycloadditions. *J. Org. Chem.* **2003**, *68*, 6153-6159. (j) Hodgson, D. M.; Selden, D. A.; Dossetter, A. G. Synthesis and Evaluation of 4,4′,6,6′-Tetrasubstituted Binaphtholphosphate Dirhodium(II) Complexes as Catalysts in Enantioselective Carbonyl Ylide Formation-Cycloaddition Reactions. *Tetrahedron: Asymmetry* **2003**, *14*, 3841-3849. (k) Hodgson, D. M.; Stupple, P. A.; Johnstone, C. Enantioselective Intramolecular 1,3-Dipolar Cycloadditions of Diazocarbonyl-Derived Oxidopyryliums. *Arkivoc* **2003**, (vii), 49-58. (l) Hodgson, D. M.; Bückl, T.; Glen, R.; Labande, A. H.; Selden, D. A.; Dossetter, A. G.; Redgrave, A. J. Catalytic Enantioselective Intermolecular Cycloadditions of 2-Diazo-3,6-Diketoester-Derived Carbonyl Ylides with Alkene Dipolarophiles. *PNAS* **2004**, *101*, 5450-5454. (m) Hodgson, D. M.; Glen, R.; Redgrave, A. J. Catalytic Enantioselective Tandem Carbonyl Ylide Formation-Intramolecular Cycloaddition with Unsaturated α-Diazo-β,ε-Diketo Sulfones. *Tetrahedron: Asymmetry.* **2009**, *20*, 754-757. (n) Hodgson, D. M.; Moreno-Clavijo, E.; Day, S. E.; Man, S. An Approach to Hyperolactone C and Analogues Using Late Stage Conjugate Addition on an Oxonium Ylide-Derived Spirofuranone. *Org. Biomol. Chem.,* **2013**, *11*, 5362-5369. (o) Hrdina, R.; Guénée, L.; Moraleda, D.; Lacour, J. Synthesis, Structural Analysis, and Catalytic Properties of Tetrakis(Binaphthyl or Octahydrobinaphthyl Phosphate) Dirhodium(II,II) Complexes. *Organometallics* **2013**, *32*, 473-479. (p) Chepiga, K. M.; Qin, C.; Alford, J. S.; Chennamadhavuni, S.; Gregg, T. M.; Olson, J. P.; Davies, H. M. L. Guide to Enantioselective Dirhodium(II)-Catalyzed Cyclopropanation with Aryldiazoacetates. *Tetrahedron* **2013**, *69*, 5765-5771. (q) Liao, M.; Wang, J. Highly Efficient [2,3]-Sigmatropic Rearrangement of Sulfur Ylide Derived from Rh(II) Carbene and Sulfides in Water. *Green Chem.,* **2007**, *9*, 184-188.

(8) (a) Ren, Y.-Y.; Zhu, S.-F.; Zhou, Q.-L. Chiral Proton-Transfer Shuttle Catalysts for Carbene Insertion Reactions. *Org. Biomol. Chem.* **2018**, *16*, 3087-3094. (b) Li, Y.; Zhao, Y.-T.; Zhou, T.; Chen, M.-Q.; Li, Y.-P.; Huang, M.-Y.; Xu, Z.-C.; Zhu, S.-F.; Zhou, Q.-L. Highly Enantioselective O–H Bond Insertion Reaction of α-Alkyl- and α-Alkenyl-α-Diazoacetates with Water. *J. Am. Chem. Soc.* **2020**, *142*, 10557-10566.

(9) (a) Yang, L.-L.; Evans, D.; Xu, B.; Li, W.-T.; Li, M.-L.; Zhu, S.-F.; Houk, K. N.; Zhou, Q.-L. Enantioselective Diarylcarbene Insertion into Si–H Bonds Induced by Electronic Properties of the Carbenes. *J. Am. Chem. Soc.* **2020**, *142*, 12394-12399. (b) Han, A. C.; Xiao, L. J.; Zhou, Q. L. Construction of Ge-Stereogenic Center by Desymmetric Carbene Insertion of Dihydrogermanes. *J. Am. Chem. Soc.* **2024**, *146*, 5643-5649.

(10) (a) Davies, H. M. L.; Hansen, T. Asymmetric Intermolecular Carbenoid C–H Insertions Catalyzed by Rhodium(II) (S)-N-(p-Dodecylphenyl)Sulfonylprolinate. *J. Am. Chem. Soc.* **1997**, *119*, 9075-9076. (b) Wei, B.; Sharland, J. C.; Blackmond, D. G.; Musaev, D. G.; Davies, H. M. L. In Situ Kinetic Studies of Rh(II)-Catalyzed C–H Functionalization to Achieve High Catalyst Turnover Numbers. *ACS Catal.* **2022**, *12*, 13400-13410.

(11) (a) *Gaussian 16,* Revision A.03, M. J. Frisch, G. W. Trucks, H. B. Schlegel, G. E. Scuseria, M. A. Robb, J. R. Cheeseman, G. Scalmani, V. Barone, G. A. Petersson, H. Nakatsuji, X. Li, M. Caricato, A. Marenich, J. Bloino, B. G. Janesko, R. Gomperts, B. Mennucci, H. P. Hratchian, J. V. Ortiz, A. F. Izmaylov, J. L. Sonnenberg, D. Williams-Young, F. Ding, F. Lipparini, F. Egidi, J. Goings, B. Peng, A. Petrone, T. Henderson, D. Ranasinghe, V. G. Zakrzewski, J. Gao, N. Rega, G. Zheng, W. Liang, M. Hada, M. Ehara, K. Toyota, R. Fukuda, J. Hasegawa, M. Ishida, T. Nakajima, Y. Honda, O. Kitao, H. Nakai, T. Vreven, K. Throssell, J. A. Montgomery, Jr., J. E. Peralta, F. Ogliaro, M. Bearpark, J. J. Heyd, E. Brothers, K. N. Kudin, V. N. Staroverov, T. Keith, R. Kobayashi, J. Normand, K. Raghavachari, A. Rendell, J. C. Burant, S. S. Iyengar, J. Tomasi, M. Cossi, J. M. Millam, M. Klene, C. Adamo, R. Cammi, J. W. Ochterski, R. L. Martin, K. Morokuma, O. Farkas, J. B. Foresman, and D. J. Fox, *Gaussian, Inc., Wallingford CT*, **2016**.

(12) (a) Hay, P. J.; Wadt, W. R. Ab initio Effective Core Potentials for Molecular Calculations. Potentials for the Transition Metal Atoms Sc to Hg. *J. Chem. Phys.* **1985**, *82*, 270-283. (b) Hay, P. J.; Wadt, W. R. Ab Initio Effective Core Potentials for Molecular Calculations. Potentials for K to Au Including the Outermost Core Orbitals. *J. Chem. Phys.* **1985**, *82*, 299-310. (c) Wadt, W. R.; Hay, P. J. Ab Initio Effective Core Potentials for Molecular Calculations. Potentials for Main Group Elements Na to Bi. *J. Chem. Phys.* **1985**, *82*, 284-298. (d) Becke, A. D. Density-Functional Exchange-Energy Approximation with Correct Asymptotic Behavior. *Phys. Rev. A* **1988,** *38*, 3098-3100. (e) Lee, C.; Yang, W.; Parr, R. G. Development of The Colle-Salvetti Correlation-Energy Formula into a Functional of the Electron Density. *Phys. Rev. B* **1988,** *37*, 785-789. (f) Becke, A. D. A New Mixing of Hartree–Fock and Local Density - Functional Theories. *J. Chem. Phys.* **1993,** *98*, 1372-1377. (g) Grimme, S., Hansen, A., Brandenburg, J. G. &

Bannwarth, C. Dispersion-Corrected Mean-Field Electronic Structure Methods. *Chem. Rev.* **116**, 5105-5154 (2016). (g) Grimme, S.; Antony, J.; Ehrlich, S.; Krieg, H. A Consistent and Accurate Ab Initio Parametrization of Density Functional Dispersion Correction (DFT-D) for the 94 Elements H-Pu. *J. Chem. Phys.* **2010,** *132*, 154104-154122. (i) Becke, A. D.; Johnson, E. R. A Density-Functional Model of the Dispersion Interaction. *J. Chem. Phys.* **2005,** *123*, 154101-154106. (j) Becke, A. D.; Johnson, E. R. Exchange-Hole Dipole Moment and the Dispersion Interaction. *J. Chem. Phys.* **2005,** *122*, 154104-154109. (h) Johnson, E. R.; Becke, A. D. A Post-Hartree-Fock Model of Intermolecular Interactions: Inclusion of Higher-Order Corrections. *J. Chem. Phys.* **2006,** *124*, 174104-174112. (l) Barone, V.; Cossi, M. Quantum Calculation of Molecular Energies and Energy Gradients in Solution by a Conductor Solvent Model. *J. Phys. Chem. A* **1998,** *102*, 1995-2001. (m) Cossi, M.; Rega, N.; Scalmani, G.; Barone, V. Energies, Structures, and Electronic Properties of Molecules in Solution with the C-PCM Solvation Model. *J. Comput. Chem.* **2003,** *24*, 669-681.

(13) For examples of other studies describing the importance of weak interaction in defining the structure of dirhodium and related catalysts, see: (a) Buchsteiner, M.; Singha, S.; Decaens, J.; Fürstner, A. Chiral Bismuth-Rhodium Paddlewheel Complexes Empowered by London Dispersion: The C–H Functionalization Nexus. *Angew. Chem. Int. Ed.* **2022**, *61*, e202212546. (b) Guo, W. T.; Tantillo, D. J. Running Wild through Dirhodium Tetracarboxylate-Catalyzed Combined CH(C)-Functionalization/Cope Rearrangement Landscapes: Does Post-Transition-State Dynamic Mismatching Influence Product Distributions? *J. Am. Chem. Soc.* **2024**. DOI: 10.1021/jacs.4c00382.

(14) Cui, Y.; Evans, O. R.; Ngo, H. L.; White, P. S.; Lin, W. Rational Design of Homochiral Solids Based on Two-Dimensional Metal Carboxylates. *Angew. Chem. Int. Ed.* **2002**, *41*, 1159-1162.

(15) Guptill, D. M.; Davies, H. M. L. 2,2,2-Trichloroethyl Aryldiazoacetates as Robust Reagents for the Enantioselective C–H Functionalization of Methyl Ethers. *J. Am. Chem. Soc.* **2014**, *136*, 17718-17721.

(16) Wei, B.; Sharland, J. C.; Lin, P.; Wilkerson-Hill, S. M.; Fullilove, F. A.; McKinnon, S.; Blackmond, D. G.; Davies, H. M. L. In Situ Kinetic Studies of Rh(II)-Catalyzed Asymmetric Cyclopropanation with Low Catalyst Loadings. *ACS Catal.* **2020**, *10*, 1161-1170.

TOC